ChemComm

Accepted Manuscript

This is an *Accepted Manuscript*, which has been through the Royal Society of Chemistry peer review process and has been accepted for publication.

Accepted Manuscripts are published online shortly after acceptance, before technical editing, formatting and proof reading. Using this free service, authors can make their results available to the community, in citable form, before we publish the edited article. We will replace this *Accepted Manuscript* with the edited and formatted *Advance Article* as soon as it is available.

You can find more information about *Accepted Manuscripts* in the **Information for Authors**.

Please note that technical editing may introduce minor changes to the text and/or graphics, which may alter content. The journal's standard **Terms & Conditions** and the **Ethical guidelines** still apply. In no event shall the Royal Society of Chemistry be held responsible for any errors or omissions in this *Accepted Manuscript* or any consequences arising from the use of any information it contains.

Journal Name

COMMUNICATION

On the Antibacterial Mechanism of Graphene Oxide (GO) Langmuir-Blodgett Films

J. D. Mangadlao, [a] C. M. Santos, [b] M. J. L. Felipe,[c] A. C. C. de Leon, [a] D. F. Rodrigues [b] and R. C. Advincula [a]*

Langmuir-Blodgett (LB) technique was used to immobilize flat graphene oxide (GO) sheets on PET substrate to ascertain as to whether the edges of GO play an integral part in its antimicrobial mechanism. The observed antibacterial activity suggests that contact to the edges is not a fundamental part of the mechanism.

Since its discovery in 2004, graphene, a two-dimensional, one-atom thick carbon nanomaterial continues to be the subject of much research worldwide. Its intriguing and extraordinary electronic properties boosted tremendous investigation from the scientific community that eventually hailed it as the future of flexible electronic displays and devices.[1] Through the years, its applications have encompassed a myriad of scientific disciplines such as high-performance nanocomposites, printed electronics, supercapacitors, chemical sensors, gas barriers and biomaterials.[2] The latter includes applications in gene and drug delivery, cancer treatment, cell growth control, stem cell differentiation, FET-based biosensors and as antimicrobials.

Several studies have shown that graphene and derivatives exhibit antimicrobial potency. Particularly, graphene oxide (GO), a heavily oxidized derivative of graphene contains various oxygen-rich functionalities that impart excellent solution processability and sites for further chemical modification, thereby facilitating its applications in many areas especially in biomedicine. Our group has earlier reported a considerable number of literature on the cytotoxicity and antimicrobial effect of graphene, GO nanocomposites and derivatives.[3] Also, several groups have shown that decorating nanoparticles on the surface of GO further improves its antimicrobial effect.[4] However, the mechanism by which pure graphene and graphene oxide act as antimicrobial remains as an unfinished business and continues to be a subject of debate.

One of the earliest reports of graphene's antimicrobial effect is on free standing graphene-based antibacterial paper that effectively inhibits E. coli.[5] While the production of graphene paper is relatively simple, the non-transparent nature of the final product as well as the huge amount of graphene required, compromises its practical applications. Generally, it is believed that the antimicrobial action of GO is due to physical and chemical factors.[5,6] The former is mechanical in nature, which mainly involves the "sharp" edges of the graphene nanosheets cutting through the bacterium's cell membrane causing intracellular matrix to leak, eventually leading to the bacterium's death (Fig. 1a). A wrapping mechanism of larger GO sheets preventing the bacterium proliferation was also reported. On the other hand, the chemical factor involves the overproduction of reactive oxygen species (ROS) that was later found to oxidize fatty acids leading to the production of lipid peroxides that stimulates a chain reaction, eventually leading to the disintegration of cell membrane followed by cell death.
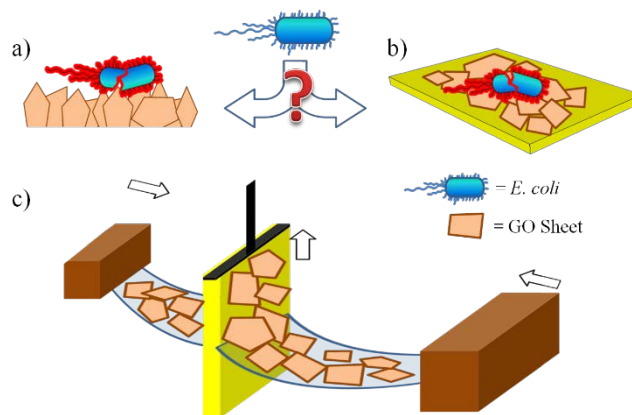
Fig. 1 a) One of the proposed models for the antibacterial mechanism of graphene/GO. b) Observed antibacterial activity of GO-LB films. c) LB set-up (arrows indicate the direction of barriers and substrate during deposition)

However, very recently, a controversial report suggested that the antibacterial activity does not stem from ROS but through the electron transfer from the bacterial membrane to the graphene surface.[7] When in contact with bacteria, graphene acts as electron acceptor that pumps the electron away from the bacterium's membrane creating an ROS-independent oxidative stress. This suggests that the surface of graphene is primarily responsible for

antimicrobial activity and not the edges. This was further supported by a more recent literature showing that bare GO kills bacteria while masking the basal plane of GO renders it inactive.[8] However, since the experiment was performed in solution, it is difficult to completely rationalize that the antimicrobial effect is only due to the basal planes because of two possible scenarios: (1) the masking may be too thick that the edges may have difficulty in penetrating the bacterial membrane and (2) the masking could have imparted rigidity to the nano-sheets preventing it from wrapping around the bacteria. In order to isolate these factors, we utilized the Langmuir-Blodgett (LB) deposition, an established technique known to deposit flat and large area GO.[9,10] Depositing GO by LB (GO-LB) means that the entire sheet including the edges are immobilized on the substrate, preventing them from puncturing and wrapping the bacteria. A standard antimicrobial assay will then determine if indeed the base planes of GO are responsible for its observed antimicrobial activity.
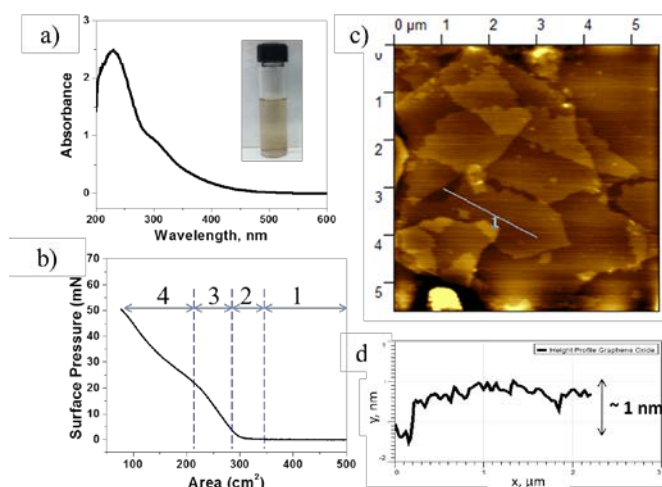

Fig. 2 a) UV-Vis absorption spectrum of GO in deionized water (inset). b) π-area isotherm of 2 mL GO dispersed in 1:5 water: methanol mixture to a final concentration of 1 mg/mL. c) AFM topography image of flat GO-LB film showing fully exfoliated sheets that are approximately 1 nm in thickness (d).

The GO was synthesized by chemical exfoliation of graphite using the classic modified Hummers and Offeman's method. The final product was characterized by UV-Vis spectroscopy where a maximum peak appeared at 231 nm and a shouldering band at 300 nm which corresponds to the $\pi-\pi*$ transitions of aromatic C=C bonds and the $n-\pi*$ transitions of C=O moieties,[11] respectively (Fig. 2a). Atomic force microscopy (AFM) and scanning electron microscopy (SEM) was performed in order to confirm the orientation of GO with respect to the substrate. Figure 2c displays the topography image of flat GO-LB films showing fully exfoliated sheets that are approximately 1 nm in thickness. The SEM images of GO-LB films are presented in Fig. S1. The GO and the GO-LB films were further characterized by attenuated total reflectance infrared (ATR-IR) spectroscopy (Fig. S2, ESI) and x-ray photoelectron spectroscopy (XPS).

GO's solution processability makes it ideal for LB deposition. The method offers the advantage of controlled deposition in a layer-by-layer fashion where the thickness of GO film can be accurately controlled upon repeated deposition. Results of our LB experiments revealed that 2 mL of sample loading is sufficient to obtain a classic π-area isotherm upon lateral compression (Fig. S3, ESI). Previous reports[10] used up to 12 mL sample loading that is of the same GO concentration and solvent as in our experiment thus, our experimental method appears to be a better alternative. Looking at the

π-area isotherm (Fig. 2b), it is evident that the GO is surface-active at the air-water interface. As the barrier was closed, a gradual increase in surface pressure was observed. There is an initial gas phase where the surface pressure essentially remained constant. As the area was further decreased, the GO sheets were pushed closer to each other resulting to the slight darkening of the monolayer due to the build-up of material density at the air-water interface. The shape of the isotherm (Figure 2 b) is similar to the reported literatures with four distinct regions corresponding to isolated flat GO sheets (1), close-packed GO (2), over-packed GO with folded edges (3) and over-packed GO with folded edges and overlapping on top of another (4).[10] At 40 mN/m, we transferred the film upstroke onto an O2 plasma-treated poly(ethylene terephthalate) (PET) substrate as we deem transparent microbe-resistant packaging materials as one of the feasible applications.
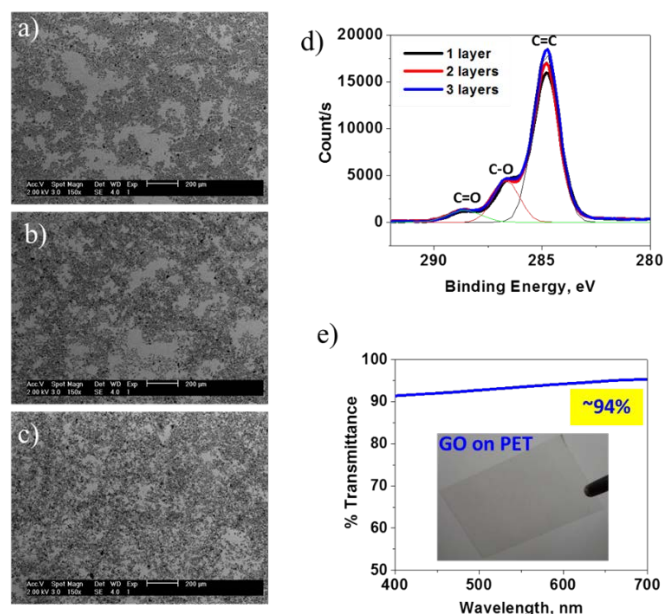

Fig. 3. a-c) Wide-area SEM image of 1, 2 and 3 layers of GO-LB. d) C1s high resolution XPS scan of GO-LB films. Deconvoluted regions show the signature binding energies of C=C, C-O and C=O moieties present in GO.[12] e) Optical transparency and photograph (inset) of 3-layer GO-LB. Scale bars in a-c represent 200 μm.

To demonstrate efficient control of material coverage, repeated deposition was performed. XPS analysis of C1s spectra of LB-GO shows increased intensity as single, double and triple layers of GO was deposited onto the substrate signifying that more material is deposited as the number of layers is increased (Fig. 3d). This is further evidenced by the wide-area SEM images depicting increased coverage and increased material density (Figure 3 a-c). Moreover, the UV-Vis spectra of the GO-LB samples also exhibited increased absorbance with increasing number of layers (Fig, S4, ESI). We examined the optical transparency of GO-LB films by measuring the light transmittance at the visible range (400 nm to 700 nm). We observed 94% transmittance for 3-layer GO-LB films. This is slightly higher compared to the reported value for 3-layer of pristine graphene (~93%).[13] The slight difference can be accounted from the fact that GO is more transparent than pristine graphene due to the disruption of the conjugation of graphene during the oxidation process.[14]

The antibacterial activity of the GO-LB films against E. coli K12 MG1655 strain was then assessed by performing *in situ* live and dead assay. The films were innoculated with 10^7cfu/mL of the bacterial solution and incubated for 2 h. Afterwhich, the films were

stained with flourescent SYTO 9 dye to show both live and dead bacteria and propidium iodide to show bacteria with compromised membranes. The ratio of dead bacteria against the total number of bacteria determines the % inactivation. All assays of the GO-LB films were performed in quadruplicates to ensure statistical significance. Results of the assay revealed that GO-LB films exhibited antibacterial efficacy which increases as the number of layers are increased. Three layers of GO displayed the most efficacy (89%) as this film contains more coverage and material density as evidenced by SEM, UV-Vis absorption and XPS analysis. As the number of layers are increased, the free spaces from previous depositions are covered with more GO sheets that can inactivate more bacteria, hence the increase in antibacterial activity. Fig. 4a-c are the representative flourescence images of the antibacterial effects of GO-LB films. It should be noted that bare PET (Fig. 4d) exhibited poor antibacterial activity (13%).
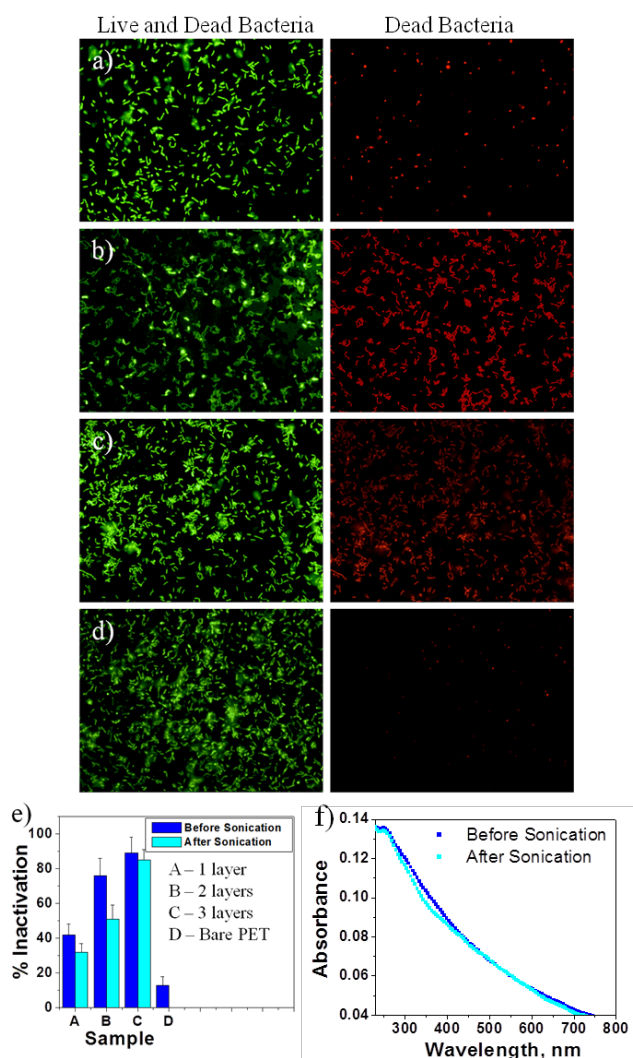
Fig. 4. Representative fluorescence images of *E. coli* on single (a), double (b), triple (c) layers of GO-LB and bare PET (d). e) Comparison of the antibacterial effect before and after ultrasonication. f) UV-Vis absorbance of 3-layer GO-LB film before and after ultrasonication.

To test the stability of the GO sheets on PET, we immersed the films in the same solvent used in preparing the solution for LB experiment (1:5 water:methanol) followed by 15-minute ultrasonication. These agitated films were also subjected to antibacterial assay. Our data revealed that the antibacterial activity of the films was retained, (Fig. 4e) but slightly lower than that of the un-sonicated films. The UV-Vis spectrum of the film after sonication (Fig. 4 f) display a very slight decrease in absorbance which may be due to the few detached GO sheets during ultrasonication, also explaining the slight decrease in antibacterial effect. The preserved antibacterial activity even after ultrasonication suggests that the GO sheets are stable on PET substrate. This stability may be due to the strong hydrogen bonding of GO to the hydroxy groups introduced to the surface of PET during O_2 plasma treatment.[15] Secondly, as the number of layers was increased by repeated deposition, the $\pi-\pi$ stacking of the GO sheets may have contributed to the observed stability (Fig. S5, ESI). The observed stability corroborates the findings of Lee et al.[16] that GO sheets tend to strongly bind onto O_2 plasma treated PET substrates due to the electrostatic interactions between the hydroxyl moieties in the basal plane of GO and the hydrophilically pre-treated PET surface.

Most importantly, the results presented herein are in agreement to the findings of Wang et al.[7] and Yang et al.[8] that the edges of GO are not an integral part of its antimicrobial mechanism. As far as our microscopy data, coupled with several other reports,[10] the GO sheets deposited by LB are immobilized and lies flat onto the substrate's surface. If the bacterial contact to the sharp edges of GO is a fundamental part of the mechanism, the antibacterial effect of GO-LB films should have not been observed. The positive correlation between the number of basal planes (by increasing the number of LB layers) and antimicrobial activity further indicates that the mechanical action of the edges are unlikely. Our findings suggest that the antimicrobial mechanism of GO primarily relies on its basal plane where different modes of bacterial inactivation can occur. This result leads us to infer that the chemistry of the functionalities tethered to the basal plane of GO should be the focus for mechanistic studies that are to be conducted in the future.

In summary, a simple route to fabricating stable, transparent and antibacterial GO films by LB technique was demonstrated and the observed antibacterial activity is layer dependent. Our results also suggest that the existing model for antibacterial mechanism of GO needs revisiting as this has important implications in the design and fabrication of antibacterial coatings and related applications.

Notes and references

[a] Department of Macromolecular Science and Engineering, Case Western Reserve University, Cleveland, Ohio 44106. E-mail: rca41@case.edu.

[b] Department of Civil and Environmental Engineering, University of Houston, Houston, TX 77204.

[c] Department of Chemistry, University of Houston, Houston, TX 77204

1. J. Lee, T.J. Ha, H. Li, K. Parrish, M. Holt, A. Dodabalapur, R. Ruoff, and D. Akinwande, *ACS Nano,* **7**, 7744.
2. V. Mittal, *Macromol. Mater. Eng.*, 2014, **299**, 906; E. Secor, P. Prabhumirashi, K. Puntambekar, M. Geier and M. Hersam, *J. Phys. Chem. Lett*., 2013, **4**, 1347; Y. Huang, J. Liang and Y. Chen, *Small*, 2012, **8**, 1805. F. Yavari and N. Koratkar, *J. Phys. Chem. Lett.*, 2012, **3**, 1746; B. M. Yoo, H. J. Shin, H. W. Yoon and H. B. Park, *J Appl Poly Sci*, 2014, **131**, 39628; C. Chung, Y.K. Kim, D. Shin, S.R. Ryoo, B. H. Hong and D.H. Min, *Acc. Chem. Res.*, 2013, **46**, 2211.

3. C. Santos, J. Mangadlao, F. Ahmed, A. Leon, R. Advincula and D. Rodrigues, *Nanotechnology*, 2012, **23**, 395101; I. M. Carpio, J. Mangadlao, H. Nguyen, R. Advincula, D. Rodrigues, *Carbon*, 2014, **77**, 289; C. Santos, M.C. Tria, R.A.M. Vergara, F. Ahmed, R. Advincula and D. Rodrigues, *Chem. Commun.*, 2011, **47**, 8892.

4. W.P. Xu, L.C. Zhang, J.P. Li, Y. Lu, H.H. Li, Y.N. Ma and W.D.Wang, *J. Mater. Chem.*, 2011, **21**, 4593; J. Tang, Q. Chen, L. Xu, S. Zhang, L. Feng, L. Cheng, H. Xu, Z. Liu and R. Peng, *ACS Appl. Mater. Interfaces*, 2013, **5**, 3867; H. Wang, J. Liu, X. Wu, Z. Tong and Z. Deng, *Nanotechnology*, 2013, **24**, 205102.

5. W. Hu, C. Peng, W. Luo, M. Lv, X. Li, D. Li, Q. Huang and C. Fan, *ACS Nano*, 2010, **4**, 4317.

6. O. Akhavan and E. Ghaderi, *ACS Nano*, 2010, **4**, 5731; S. Liu, T. H. Zeng, M. Hofmann, E. Burcombe, J. Wei, R. Jiang, J. Kong and Y. Chen, *ACS Nano*, 2011, **5,** 6971; O. Akhavan, E. Ghaderi and A. Esfandiar, *J. Phys. Chem. B*, 2011, **115**, 6279; K. Krishnamoorthy, M. Veerapandian, L.H. Zhang, K. Yun and S.J. Kim, *J. Phys. Chem. C*, 2012, **116**, 17280; S. Liu, M. Hu, T.H. Zeng, R. Wu, R. Jiang, J. Wei, L. Wang, J. Kong and Y. Chen, *Langmuir*, 2012, **28**, 12364; Y. Tu, M. Lv, P. Xiu, T. Huynh, M. Zhang, M. Castelli, Z. Liu, Q. Huang, C. Fan, H. Fang, R. Zhou, *Nat. Nanotechnol,* 2012, **8**, 594; Y. Li, H. Yuan, A. Bussche, M. Creighton, R. Hurt, A. Kane and H. Gaoa, *PNAS*, 2013, **110**, 12295.

7. J. Li, G. Wang, H. Zhu, M. Zhang, X. Zheng, Z. Di, X. Liu and Xi Wang, *Scientific Reports*, 2014, **4**, 4359.

8. L. Hui, J.G. Piao, J. Auletta, K. Hu, Y. Zhu, T. Meyer, H. Liu, L. Yang, *ACS Appl. Mater. Interfaces*, 2014, **6**, 13183.

9. X. Li, G. Zhang, X. Bai, X. Sun, X. Wang, E. Wang and H. Dai, *Nat. Nanotechnol.* 2008, **3**, 538.

10. L. Cote, F. Kim and J. Huang, *J. Am. Chem. Soc*., 2009, **131**, 1043; Q. Zheng, W. H. Ip, X. Lin, N.Yousefi, K. K. Yeung, Z. Li and Jang-Kyo Kim, *ACS Nano*, 2011, **5**, 6039.

11. J. Paredes, S. Villar-Rodil, A. Martinez-Alonzo, M. Tasco, *Langmuir*, 2008, **24**, 10560.

12. H. Li, S. Pang, S. Wui, X. Feng, K. Mullen, C. Bubeck*, J. Am. Chem. Soc.* 2011, **133**, 9423.

13. R. Nair, P. Blake, A. Grigorenko, K. Novoselov, T. Booth, T. Stauber, N. Peres, A. Geim, *Science* 2008, **320**, 1308; X. Li, Y. Zhu, W. Cai, M. Borysiak, B. Han, D. Chen. R. Piner, L. Colombo, R. Ruoff, *Nano Lett.,* 2009, **9**, 4539.

14. O. O. Ekiz, M. Urel, H. Güner, A. K. Mizrak, A. Dana, *ACS Nano* 2011, **5**, 2475.

15. M. Nie, P. Patel, K. Sun, D. D. Meng, Superhydrophilic Anti-Fog Polyester Film by Oxygen Plasma Treatment. Paper presented at Nano/Micro Engineered and Molecular Systems, 2009 at Shenzhen; P. Patel, C. Choi, D. D. Meng, *J. Lab. Autom.,* 2010, **15**, 114.

16. I. K. Moon, J. I. Kim, H. Lee, K. Hur, W. C. Kim, H. Lee, *Scientific Reports*, 2012, **3**, 112.